Chaos, chaos control and synchronization of the vibrometer system

Z-M Ge, C-C Lin and Y-S Chen

Proceedings of the Institution of Mechanical Engineers, Part C: Journal of Mechanical Engineering Science 2004 218: 1001
DOI: 10.1243/0954406041991206

Chaos, chaos control and synchronization of the vibrometer system

Z-M Ge*, **C-C Lin** and **Y-S Chen**
Department of Mechanical Engineering, National Chiao Tung University, Hsinchu, Taiwan, Republic of China

Abstract: The dynamic system of the vibrometer is shown to produce regular and chaotic behaviour as the parameters are varied. When the system is non-autonomous, the periodic and chaotic motions are obtained by numerical methods. Many effective methods have been used in chaos synchronization. It has been shown that chaos can be synchronized using special feedback control and that external excitations affect the synchronization.

Keywords: bifurcation, chaos, chaos control, chaos synchronization, vibrometer system

1 INTRODUCTION

During the past two decades, many studies have shown that chaotic phenomena are observed in many physical systems that possess non-linearity [**1**–**4**]. It was also reported that the chaotic motion occurred in many non-linear control systems [**5**, **6**].

In nature, most physical systems are non-linear and can be described by the non-linear equations of motion, which in general cannot be linearized. Hence, research into non-linear systems has spread quickly. For the non-linear system, the study of the types of periodic solution, the effects to the solutions caused by different parameters and initial conditions and the stability analysis of the solutions comprise the major tasks. The central characteristics are that a process such as randomization happens in the deterministic system and small differences in the initial conditions produce very large ones in the final phenomena. The irregular and unpredictable motions of many non-linear systems have been labelled 'chaotic'. A large number of studies on chaotic behaviour has been undertaken up to now.

An earthquake is one of the largest natural disasters. Therefore measurement of an earthquake is extremely important. The vibrometer is a useful and convenient tool to do this.

The MS was received on 22 April 2003 and was accepted after revision for publication on 28 May 2004.
* *Corresponding author: Department of Mechanical Engineering, National Chiao Tung University, 1001 Ta Hsueh Road, Hsinchu 30050, Taiwan, Republic of China.*

The aim of this paper is to present the stability, chaos, chaos control and synchronization of a vibrometer. Many modern techniques are used in analysing deterministic non-linear system behaviour. In section 2, the governing equations of motion will be formulated. In section 3, bifurcation diagrams, phase portraits, the Poincaré map and Lyapunov exponents are presented. In section 4, the time history and power spectrum are given. In section 5, attention is shifted to controlling chaos [**7**]. In order to improve the performance of a dynamic system or avoid chaotic phenomena, a chaotic system for periodic motion that is beneficial in working with a particular condition must be controlled. For this purpose, chaos control by constant torque, by periodic torque, by periodic impulse torque, delayed feedback control [**8**], optimal control [**9**], adaptive control [**10**] algorithm and periodic parametric forcing are used to control chaos.

In section 6, synchronization [**9**, **11**, **12**] of two or more dynamical systems is a fundamental phenomenon for study in science, engineering and technology. Traditionally, synchronization has been limited for periodic signals. It has now been realized that chaotic signals can also be used for synchronization. There are many effective methods that can be used for chaos synchronization. Synchronization of feedback methods [**13**] in the two identical non-autonomous coupled systems has been studied in this paper. Feedback synchronization and the phase effect of two external excitations to synchronization for two coupled systems are studied.

2 EQUATIONS OF MOTION

The system considered here is depicted in Fig. 1. It is assumed that viscous dampings exist. The pendulum is swinging in a vertical plane. The kinetic energy and potential energy and the Rayleigh dissipation function of the system are written as follows:

$$T = \tfrac{1}{2}m_{\mathrm{A}}\dot{x}_{\mathrm{A}}^2 + \tfrac{1}{2}m_{\mathrm{B}}\{[\dot{x}_{\mathrm{A}} - \ell\dot{\phi}\cos(\alpha+\phi)]^2 + [\ell\dot{\phi}\sin(\alpha+\phi)]^2\}$$
$$V = \tfrac{1}{2}k_\phi[\alpha_0 - (\alpha+\phi)]^2 - m_{\mathrm{B}}g\ell\cos(\alpha+\phi) + \tfrac{1}{2}k_x x_{\mathrm{A}}^2$$
$$R = \tfrac{1}{2}c_x\dot{x}^2 + \tfrac{1}{2}c_\phi\dot{\phi}^2$$

where

m_{A} = mass of the slider
m_{B} = mass of the pendulum
x_{A} = displacement of the slider
ϕ = angle between the equilibrium position and the pendulum
ℓ = length of the pendulum
c_ϕ and c_x = damping constants
k_ϕ and k_x = spring constants
α = equilibrium angle

It is easy to obtain the Lagrangian

$$L = T - V = \tfrac{1}{2}m_{\mathrm{A}}\dot{x}_{\mathrm{A}}^2 + \tfrac{1}{2}m_{\mathrm{B}}\left[(\dot{x}_{\mathrm{A}}^2 - 2\ell\dot{x}_{\mathrm{A}}\dot{\phi}\cos(\alpha+\phi) + \ell^2\dot{\phi}^2\right] - \tfrac{1}{2}k_\phi[\alpha_0 - (\alpha+\phi)]^2 + m_{\mathrm{B}}g\ell\cos(\alpha+\phi) - \tfrac{1}{2}k_x x_{\mathrm{A}}^2$$

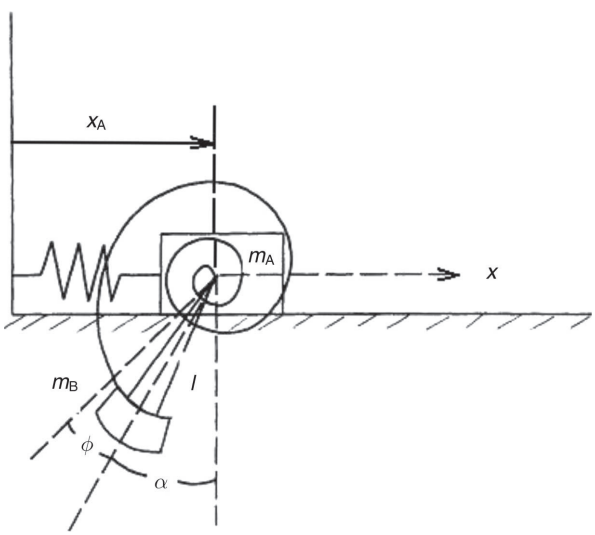

Fig. 1 Sketch of a vibrometer

Using Langrange equations,

$$\frac{\mathrm{d}}{\mathrm{d}t}\left(\frac{\partial L}{\partial \dot{x}}\right) - \frac{\partial L}{\partial x} + \frac{\partial R}{\partial \dot{x}} = 0$$
$$\frac{\mathrm{d}}{\mathrm{d}t}\left(\frac{\partial L}{\partial \dot{\phi}}\right) - \frac{\partial L}{\partial \phi} + \frac{\partial R}{\partial \dot{\phi}} = 0$$

and the equilibrium condition

$$m_{\mathrm{B}}g\ell\sin\alpha = k_\phi(\alpha_0 - \alpha)$$

gives

$$\begin{aligned}&(m_{\mathrm{A}} + m_{\mathrm{B}})\ddot{x}_{\mathrm{A}} - m_{\mathrm{B}}\ell\ddot{\phi}\cos(\alpha+\phi) + m_{\mathrm{B}}\ell\dot{\phi}^2\sin(\alpha+\phi) + k_x x_{\mathrm{A}} = -c_x\dot{x}_{\mathrm{A}}\\ &m_{\mathrm{B}}\ell^2\ddot{\phi} - m_{\mathrm{B}}\ell\ddot{x}_{\mathrm{A}}\cos(\alpha+\phi) + k_\phi\phi + m_{\mathrm{B}}g\ell[\sin(\alpha+\phi) - \sin\alpha] = -c_\phi\dot{\phi}\end{aligned} \tag{1}$$

where the variable ϕ indicates the measured quantity in the range of linear theory.

This vibrometer cannot work properly for non-linear dynamic equations (1), even where no chaotic behaviour exists. The chaotic systems have the intrinsic property sensitivity depending on initial conditions. It is therefore not possible to predict the long-time behaviour of chaotic systems. Thus the measurement of the vibrometer does not make sense if chaotic motion exists in this system.

Let $x_{\mathrm{A}}/\ell = x_1$, $\dot{x}_{\mathrm{A}}/\ell = x_2$, $\alpha + \phi = x_3'$, $\dot{\phi} = x_4$, $k_x = k_1, k_\phi = k_2, c_x = c_1, c_\phi = c_2$ and change the time-scale to dimensionless time $\tau = \Omega t$. Denote $\mathrm{d}/\mathrm{d}\tau$ also by a dot $\cdot$ for simplicity. The state equations can then be written as

$$\begin{aligned}\dot{x}_1 &= x_2\\ \dot{x}_2 &= -\frac{\sin x_3'}{a - \cos^2 x_3'}x_4^2 - \frac{g\cos x_3'(\sin x_3' - \sin\alpha)}{\Omega^2\ell(a - \cos^2 x_3')} - \frac{k_2(x_3' - \alpha)\cos x_3'}{\Omega^2 m_{\mathrm{B}}\ell^2(a - \cos^2 x_3')} - \frac{k_1}{\Omega^2 m_{\mathrm{B}}(a - \cos^2 x_3')}x_1\\ &\quad - \frac{c_1}{\Omega m_{\mathrm{B}}(a - \cos^2 x_3')}x_2 - \frac{c_2\cos x_3'}{\Omega m_{\mathrm{B}}\ell^2(a - \cos^2 x_3')}x_4\\ \dot{x}_3 &= x_4\\ \dot{x}_4 &= -\frac{\sin x_3'\cos x_3'}{a - \cos^2 x_3'}x_4^2 - \frac{ag(\sin x_3' - \sin\alpha)}{\Omega^2\ell(a - \cos^2 x_3')} - \frac{ak_2(x_3' - \alpha)}{\Omega^2 m_{\mathrm{B}}\ell^2(a - \cos^2 x_3')} - \frac{k_1\cos x_3'}{\Omega^2 m_{\mathrm{B}}(a - \cos^2 x_3')}x_1\\ &\quad - \frac{c_1\cos x_3'}{\Omega m_{\mathrm{B}}(a - \cos^2 x_3')}x_2 - \frac{ac_2}{\Omega m_{\mathrm{B}}\ell^2(a - \cos^2 x_3')}x_4\end{aligned} \tag{2}$$

where

$$a = \frac{m_{\mathrm{A}} + m_{\mathrm{B}}}{m_{\mathrm{B}}}, \qquad \Omega = \sqrt{\frac{g}{\ell}}$$

The equilibrium state of equations (1) can be found by the equilibrium condition $m_B g\ell \sin\alpha = k_\phi(\alpha_0 - \alpha)$, or by letting the right-hand side of equations (2) be zero. Unfortunately, this equation cannot be solved by elementary functions. It is often solved numerically.

3 BIFURCATION DIAGRAM, PHASE PORTRAITS, POINCARÉ MAP AND LYAPUNOV EXPONENT

Because of the given vertical vibration $A\sin\omega t$ of the horizontal basement for the Lagrange equations written in the non-inertial coordinate system fixed with the moving basement, the gravity is represented by a constant term and a harmonic term $(g + A'\omega^2 \sin\omega t)$, where g, A' and ω are constants. Then equations (2) are rewritten in the form

$$
\begin{aligned}
\dot{x}_1 &= f_1 = x_2\\
\dot{x}_2 &= f_2\\
&= -\frac{\sin x_3'}{a-\cos^2 x_3'}x_4^2 - \frac{\{g + A'\omega^2\sin[(\omega/\Omega)\tau]\}\cos x_3'(\sin x_3' - \sin\alpha)}{\Omega^2\ell(a-\cos^2 x_3')} - \frac{k_2(x_3'-\alpha)\cos x_3'}{\Omega^2 m_B\ell^2(a-\cos^2 x_3')}\\
&\quad - \frac{k_1}{\Omega^2 m_B(a-\cos^2 x_3')}x_1 - \frac{c_1}{\Omega m_B(a-\cos^2 x_3')}x_2 - \frac{c_2\cos x_3'}{\Omega m_B\ell^2(a-\cos^2 x_3')}x_4\\
\dot{x}_3 &= f_3 = x_4\\
\dot{x}_4 &= f_4\\
&= -\frac{\sin x_3'\cos x_3'}{(a-\cos^2 x_3')}x_4^2 - \frac{a\{g + A'\omega^2\sin[(\omega/\Omega)\tau]\}(\sin x_3' - \sin\alpha)}{\Omega^2\ell(a-\cos^2 x_3')} - \frac{ak_2(x_3'-\alpha)}{\Omega^2 m_B\ell^2(a-\cos^2 x_3')}\\
&\quad - \frac{k_1\cos x_3'}{\Omega^2 m_B(a-\cos^2 x_3')}x_1 - \frac{c_1\cos x_3'}{\Omega m_B(a-\cos^2 x_3')}x_2 - \frac{ac_2}{\Omega m_B\ell^2(a-\cos^2 x_3')}x_4
\end{aligned}
\tag{3}
$$

where

$$a = 2.0, g = 9.8, k_1 = 1, k_2 = 2, c_1 = 0.1, c_2 = 0.3, m_B = 2, \omega = \Omega = 1, \ell = 1, \alpha = 0.2, A = A'\omega^2.$$

The information concerning the dynamics of the non-linear system for specific values of the parameters is provided. The dynamics may be viewed more completely over a range of parameter values. As the parameter is changed, the equilibrium points can be created or destroyed, or their stability can be lost. The phenomenon of sudden change in the motion as a parameter is varied is called bifurcation and the parameter values at which they occur are called bifurcation points. The bifurcation diagram of the non-linear system of equations is depicted in Fig. 2, where $A \in [26.5, 29.2]$ with the incremental value of A as 0.01.

The phase portrait is the evolution of a set of trajectories emanating from various initial conditions in the state space. When the solution reaches stable, the asymptotic behaviours of the phase trajectories are

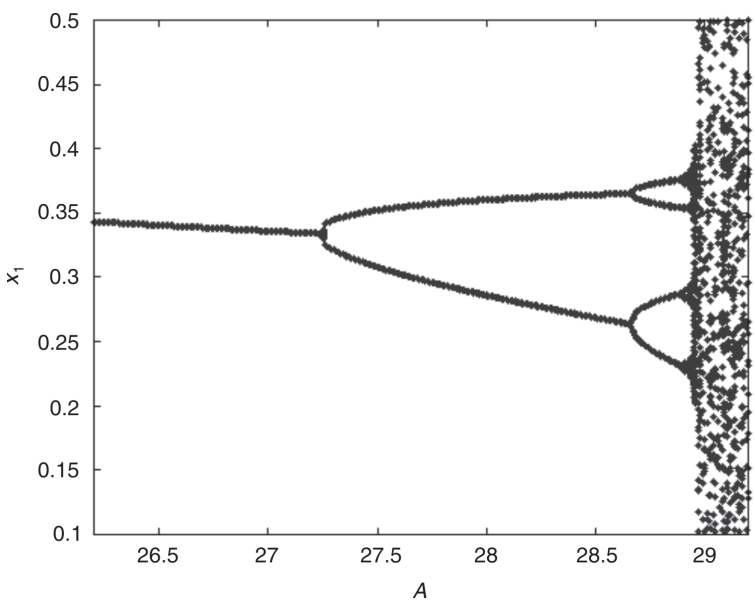

Fig. 2 Bifurcation diagram for A between 26.5 and 29.2 versus x_1

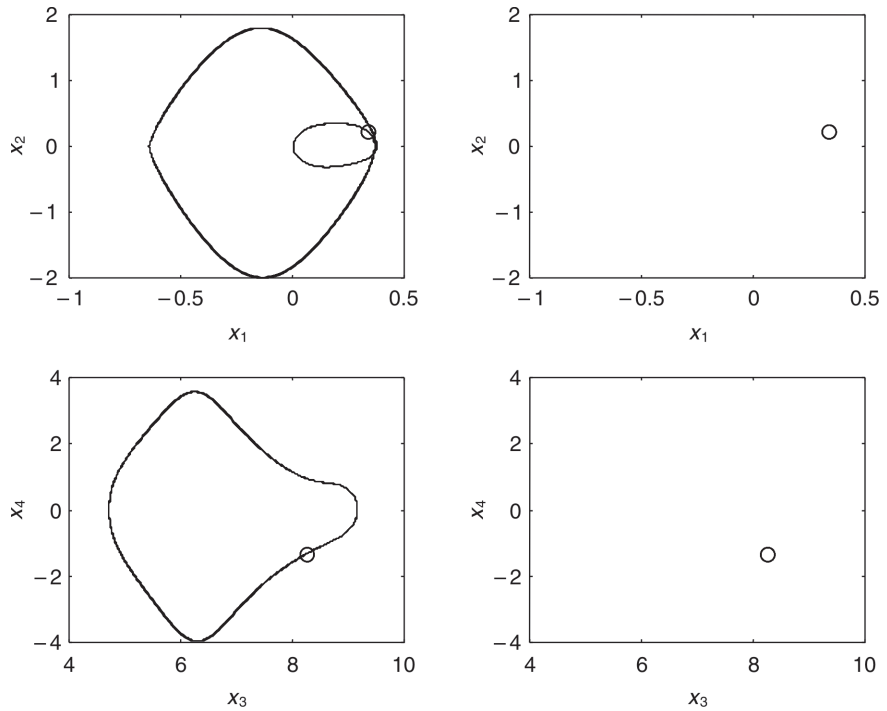

Fig. 3 Phase portraits and the Poincaré map of period 1

particularly interested and the transient behaviours in the system are neglected. The Poincaré map is a better method of displaying the dynamics. Periods 1, 2 and 4 and chaos for equations (3) are plotted in Figs 3 to 6 for $A = 27.2$, 27.3, 28.8 and 29.

The Lyapunov exponent may be used to measure the sensitive dependence on initial conditions. It is an index for chaotic behaviour. Different solutions of the dynamical system, such as fixed points, periodic motions, quasiperiodic motion and chaotic motion,

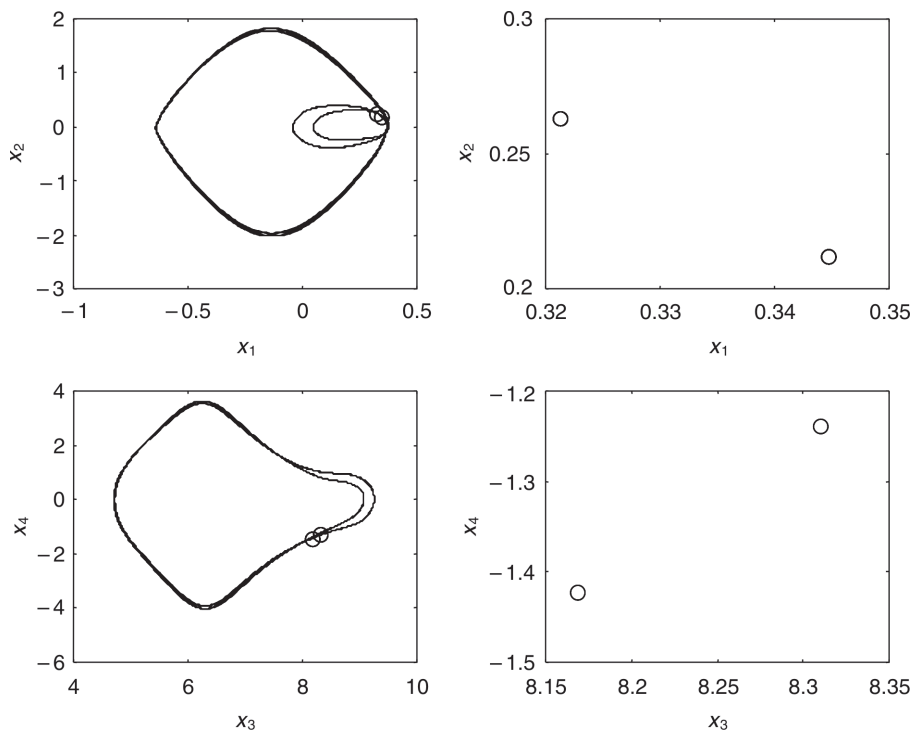

Fig. 4 Phase portraits and the Poincaré map of period 2

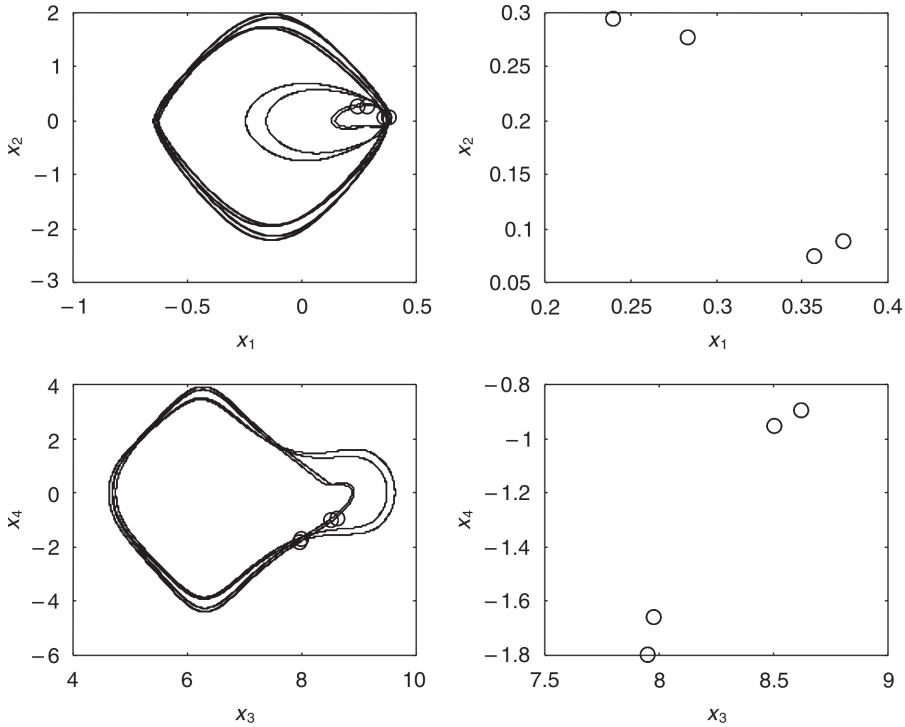

Fig. 5 Phase portraits and the Poincaré map of period 4

can be distinguished using it. If two trajectories start close to one another in phase space, they will move exponentially away from each other for small times on average. Thus, if d_0 is a measure of the initial distance between the two starting points, the distance is $d(t) = d_0 \times 2^{\lambda t}$. The symbol λ is called the Lyapunov exponent. The divergence of chaotic orbits can only be exponential locally, because if the system is bounded,

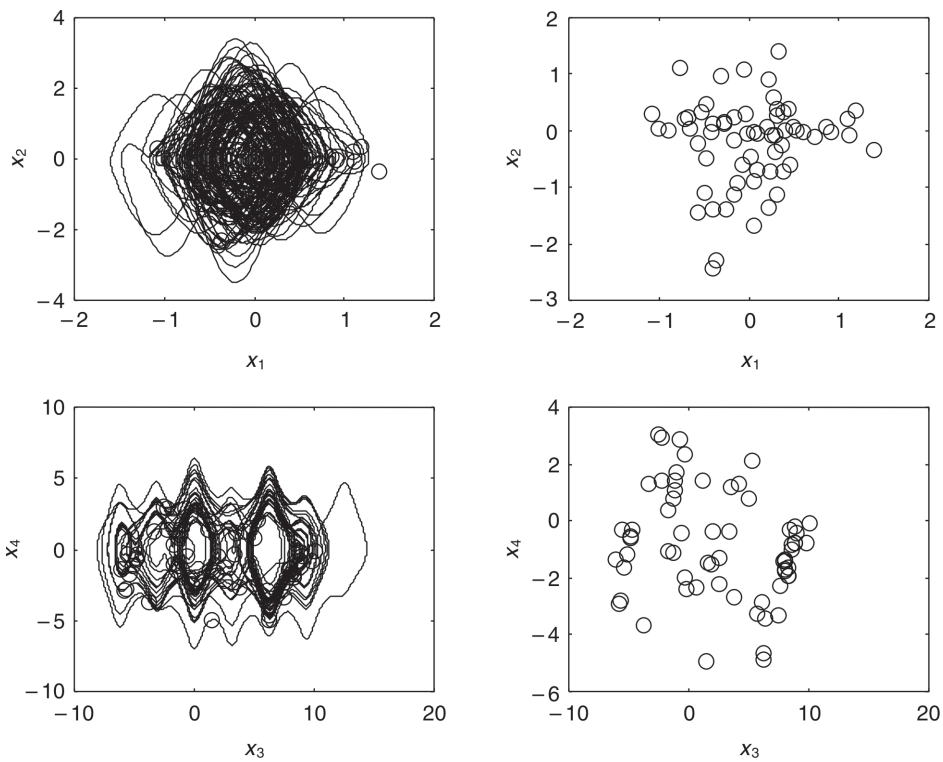

Fig. 6 Phase portraits and the Poincaré map of chaos

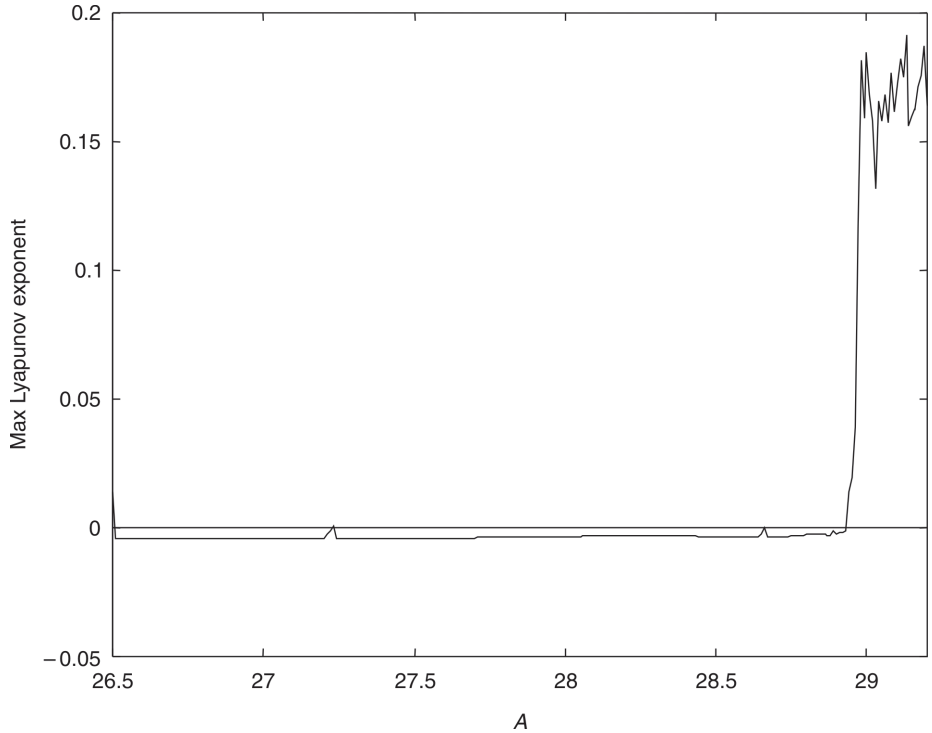

Fig. 7 The largest Lyapunov exponent for A between 26.5 and 29.2

$d(t)$ cannot grow to infinity. A measure of this divergence of orbits is that the exponential growth at many points along a trajectory has to be averaged. When $d(t)$ is too large, a new 'nearby' trajectory $d_0(t)$ is defined. The Lyapunov exponent can be expressed as:

$$\lambda = \frac{1}{t_N - t_0} \sum_{k=1}^{N} \log_2 \frac{d(t_k)}{d_0(t_k - 1)}$$

The signs of the Lyapunov exponents provide a qualitative picture of a system dynamics. The criterion is

$\lambda > 0$ (chaotic)
$\lambda \leqslant 0$ (regular motion)

The periodic and chaotic motions can be distinguished by the bifurcation diagram, while the quasiperiodic motion and chaotic motion may be confused. However, they can be distinguished by the Lyapunov exponent method. The Lyapunov exponents of the solutions of the non-linear dynamical system are plotted in Fig. 7 as $A = 26.5$–29.2.

4 TIME HISTORY AND THE POWER SPECTRUM

A useful technique for the identification and characterization of the system is the power spectrum. It is often used to distinguish between periodic, quasi-periodic and chaotic behaviours for a dynamical system [**14**]. Any function $x(t)$ may be represented as a superposition of different periodic components. The determination of their relative strength is called spectral analysis. If it is periodic, the spectrum may be a linear combination of oscillations whose frequencies are integer multiples of basic frequency. The linear combination is called a Fourier series. If it is not periodic, the spectrum must then be in terms of oscillations with a continuum of frequencies. Such a representation of the spectrum is called the Fourier integral of $x(t)$. The representation is useful for dynamical analysis. The non-autonomous system is observed by portraits of time history and the power spectrum in Figs 8 to 11 for $A = 27.2$, 27.3, 28.8, 29.

5 CONTROLLING CHAOS

Chaos has been found in many different physical systems. Analysing and predicting the behaviour of a chaotic system is beneficial, in order to maximize the benefit and thus be able to control it. Chaos control can be understood as a process or mechanism that enhances existing chaos in a dynamical system when it is useful and suppresses it when it is harmful.

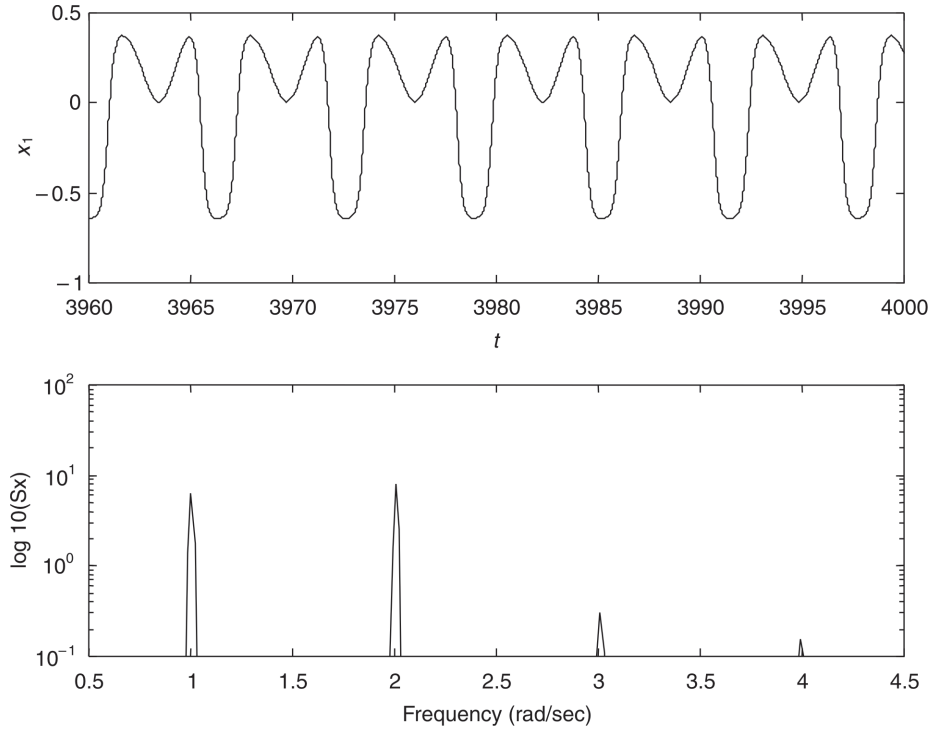

Fig. 8 Time history and the power spectrum of period 1 versus x_1

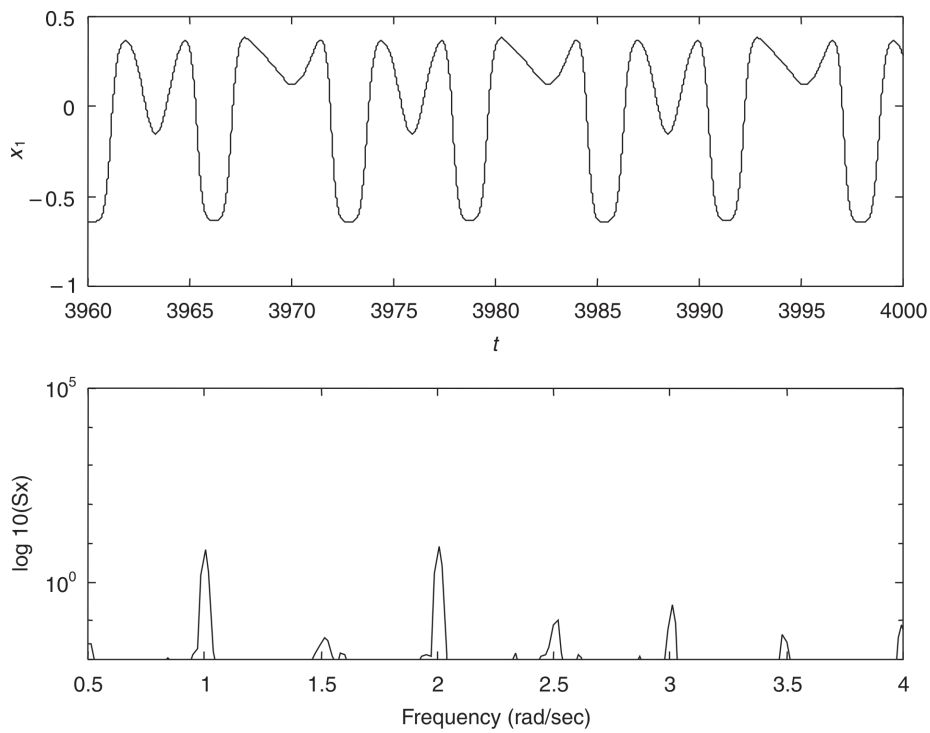

Fig. 9 Time history and the power spectrum of period 2 versus x_1

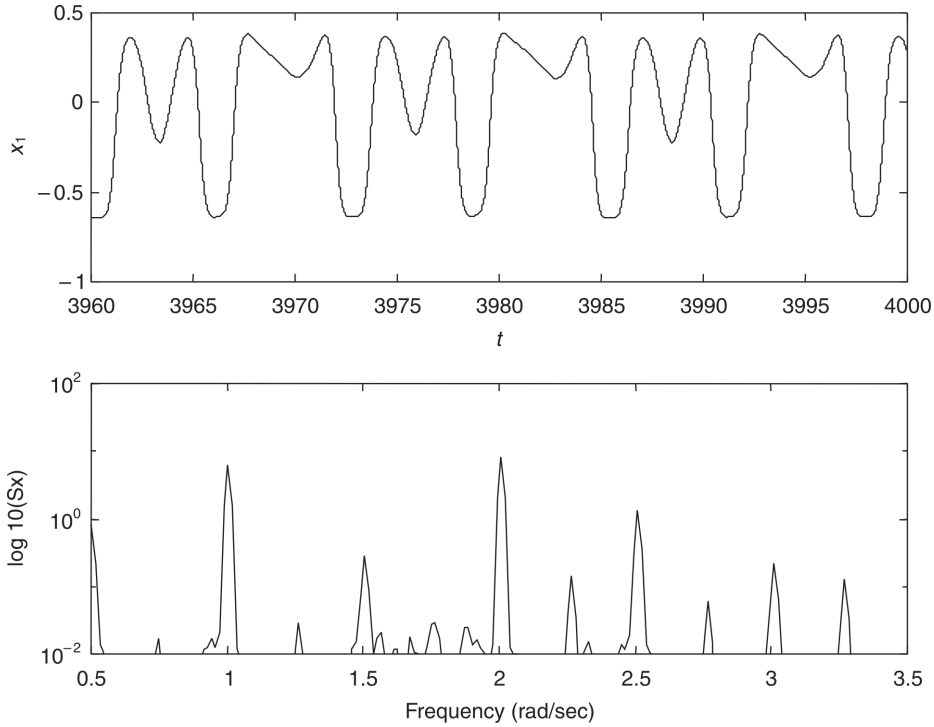

Fig. 10 Time history and the power spectrum of period 4 versus x_1

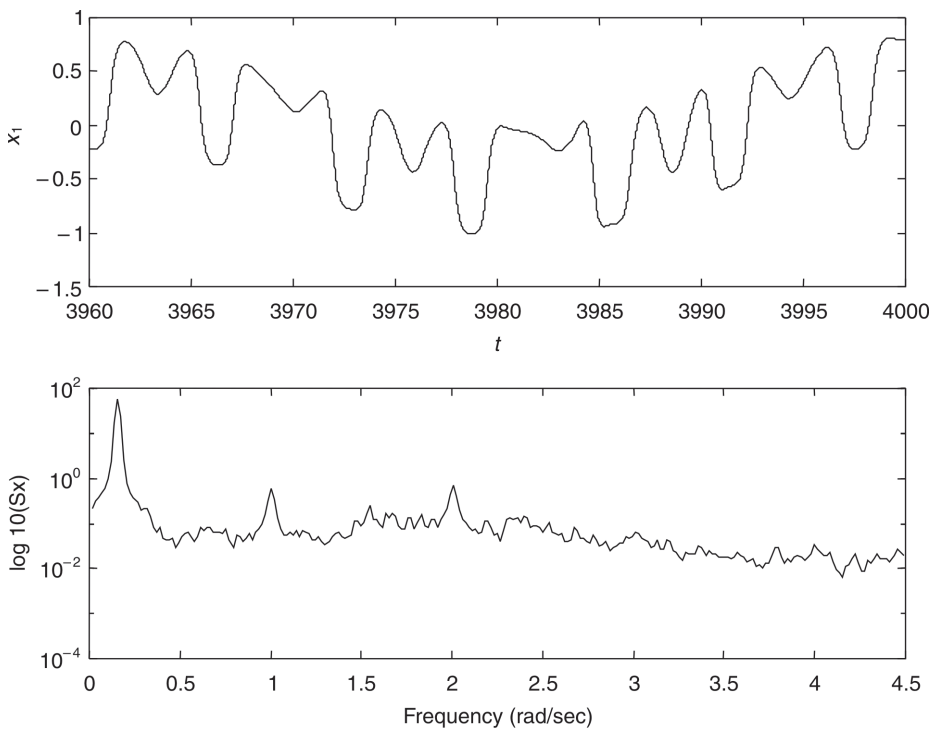

Fig. 11 Time history and the power spectrum of chaos versus x_1

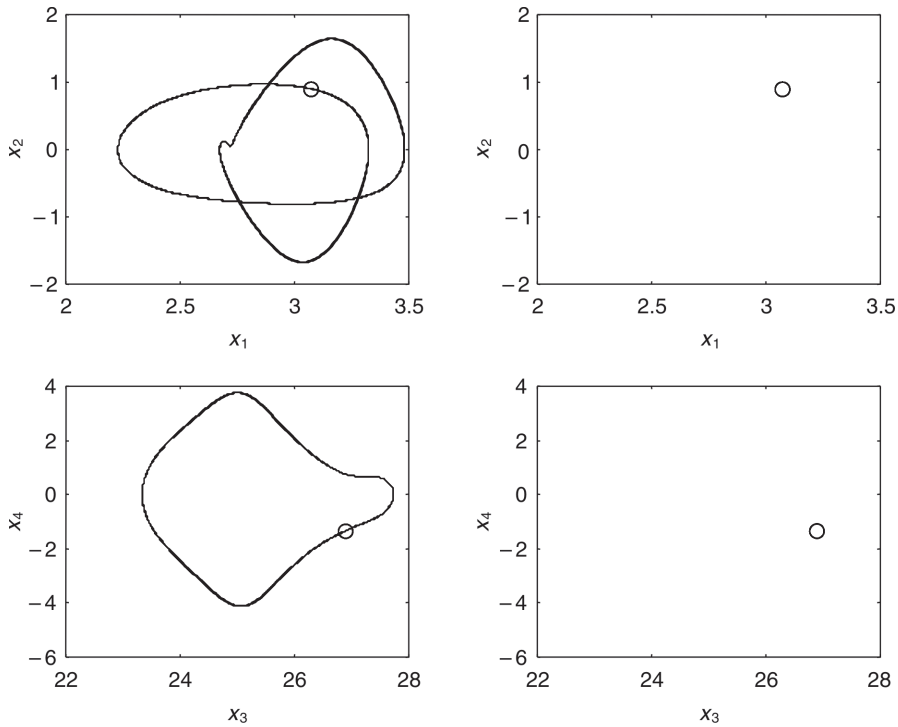

Fig. 12 Phase portraits and the Poincaré map of period 1 for $T = 2$

5.1 Controlling chaos by the addition of a constant torque

Several interesting non-linear dynamic behaviours of the system have been studied in previous sections. It was shown that the forced system exhibited both regular and chaotic motion. Converting chaotic oscillations into desired regular ones with a periodic time dependence would be beneficial in working with a particular system.

A constant term can be added when controlling chaos. The torque T is applied to the pendulum. Thus the equations become

$$\begin{aligned} \dot{x}_1 &= f_1 \\ \dot{x}_2 &= f_2 \\ \dot{x}_3 &= f_3 \\ \dot{x}_4 &= f_4 + T \end{aligned} \tag{4}$$

Increasing the torque T from zero upwards, the chaotic behaviour is changed to regular motion when $A = 28.95$. The system returns to regular motion when the magnitude of the constant torque T is large enough. It is clear that when $T = 2$, the system is in period 1, shown in Fig. 12.

5.2 Controlling chaos by the addition of periodic torque

The method of suppression of chaos by addition of a periodic force is similar to the method used in the previous section. However, $T = T_1 \sin \varpi\tau$ is used in the pendulum. Then the equations become

$$\begin{aligned} \dot{x}_1 &= f_1 \\ \dot{x}_2 &= f_2 \\ \dot{x}_3 &= f_3 \\ \dot{x}_4 &= f_4 + T_1 \sin \varpi\tau \end{aligned}$$

Here $\varpi = 1$ is fixed and T is increased from zero upwards. In Fig. 13, it is clear that the system is in period 1 when T is 1.04.

5.3 Controlling chaos by the addition of periodic impulse torque

As in section 5.2, a periodic impulse torque can also be added instead of a period torque. Consider the system of the form (4) and assume that the system is controlled by a periodic impulse input

$$T = \rho \sum_{t=0}^{\infty} \delta(\tau - \mathrm{i}\tau_\mathrm{d}) \tag{5}$$

where ρ is a constant impulse intensity, τ_d is the period between two consecutive impulses and δ is the standard Kronecker delta function.

With different values of ρ and τ_d the controlled system can be stabilized at different periodic orbits. When $\tau_\mathrm{d} = 0.1$, the appropriate parameter ρ is adjusted

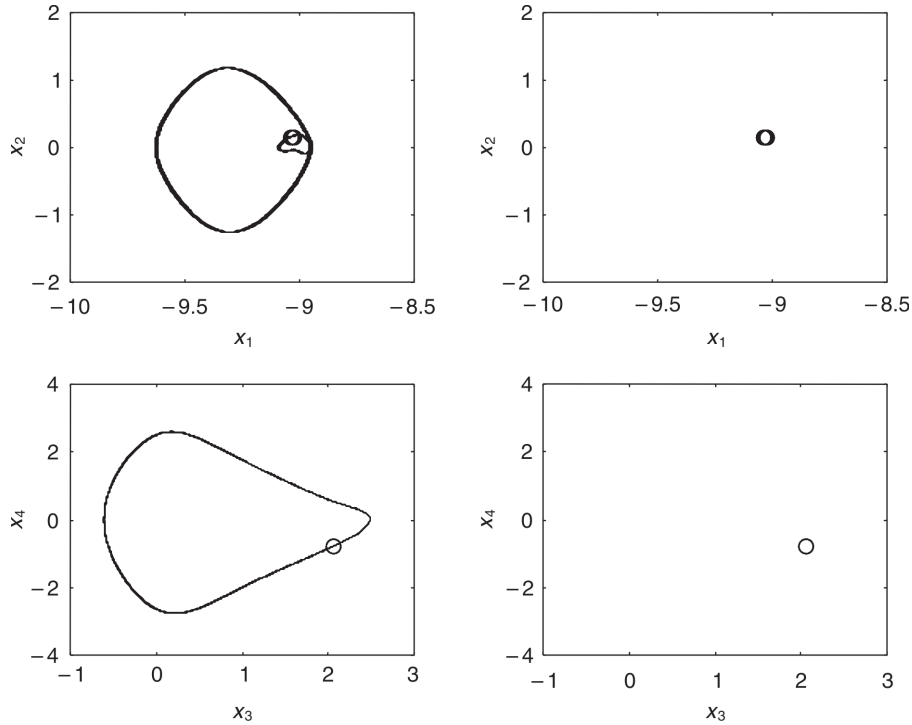

Fig. 13 Phase portraits and the Poincaré map of period 1 for $T = 1.04$

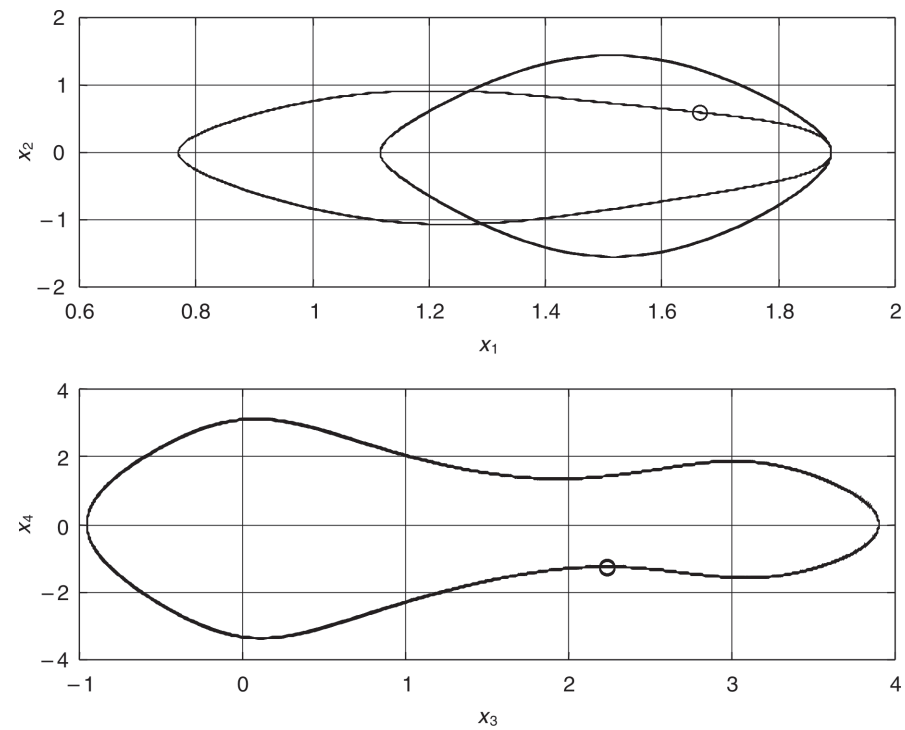

Fig. 14 Phase portraits and the Poincaré map of period 1 for $\rho = 4.2$

to be equal to 4.2 and the chaotic behaviour disappears. The results are shown in Fig. 14.

5.4 Controlling of chaos by delayed feedback control

Delayed feedback control is based on a self-controlling feedback, which combines feedback with a periodic delay of a special form. It is achieved by using the output signal, which is fed in a periodic delay time τ_d and adjusts the weight of the feedback. The controlling input has the following style:

$$u(\tau) = k[x(\tau - \tau_d) - x(\tau)]$$

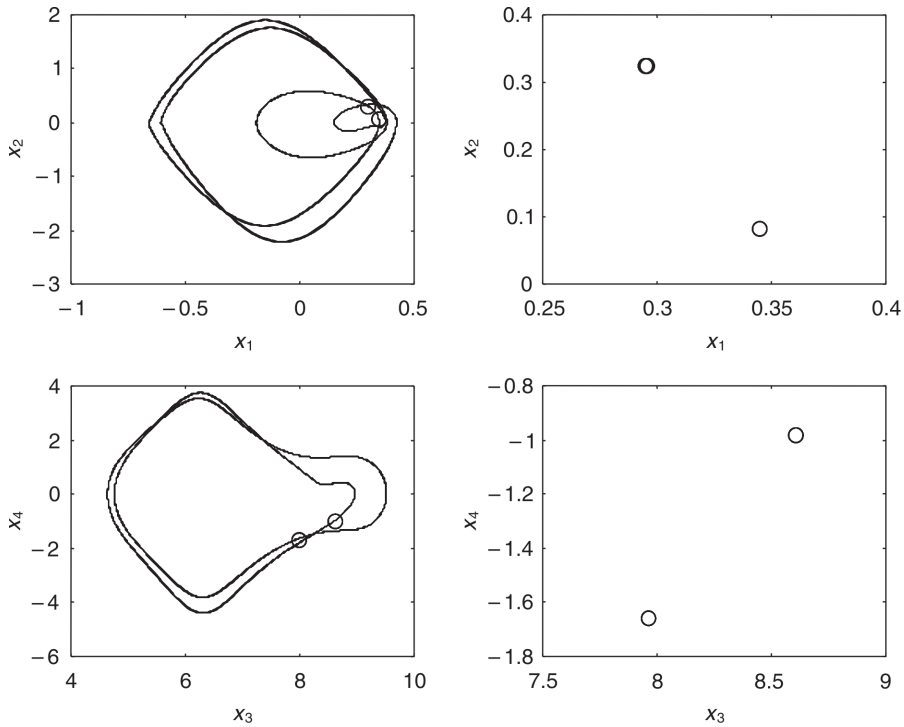

Fig. 15 Phase portraits and the Poincaré map of period 2 for $k = 1.6$

where

$k =$ an adjustable weight of the feedback
$\tau_d =$ periodic delay time
$x(\tau) =$ uncontrolled system state

Therefore the equations become

$$\dot{x}_1 = f_1$$
$$\dot{x}_2 = f_2$$
$$\dot{x}_3 = f_3$$
$$\dot{x}_4 = f_4 + u$$

Choosing an appropriate k for the feedback stabilization can be achieved. The result for period 2 with $k = 1.6, \tau_d = 0.1$ is shown in Fig. 15.

5.5 Optimal control of chaos

Optimal control is a well-established engineering control strategy and is useful for both linear and non-linear systems with linear or non-linear controllers. Optimization in control is often a main objective in engineering systems and can be used to design a bounded controller.

For the concept of optimal control, the system with a controller u is considered:

$$\begin{aligned}
\dot{x}_1' &= x_2 = f_1 \\
\dot{x}_2 &= -\frac{\sin x_3'}{a - \cos^2 x_3'} x_4^2 - \frac{g \cos x_3' (\sin x_3' - \sin \alpha)}{\Omega^2 \ell (a - \cos^2 x_3')} \\
&\quad - \frac{c(x_3' - \alpha) \cos x_3'}{\Omega^2 m_B \ell^2 (a - \cos^2 x_3')} - \frac{k_2}{\Omega m_B (a - \cos^2 x_3')} x_2 \\
&\quad - \frac{k_1 \cos x_3'}{\Omega m_B \ell^2 (a - \cos^2 x_3')} x_4 + u = f_2 \\
\dot{x}_3 &= x_4 = f_3 \\
\dot{x}_4 &= -\frac{\sin x_3' \cos x_3'}{a - \cos^2 x_3'} x_4^2 - \frac{ag(\sin x_3' - \sin \alpha)}{\Omega^2 \ell (a - \cos^2 x_3')} \\
&\quad - \frac{ac(x_3' - \alpha)}{\Omega^2 m_B \ell^2 (a - \cos^2 x_3')} - \frac{ak_1}{\Omega m_B \ell^2 (a - \cos^2 x_3')} x_4 \\
&\quad - \frac{k_2 \cos x_3'}{\Omega m_B (a - \cos^2 x_3')} x_2 = f_4
\end{aligned} \tag{6}$$

The Hamilton function is defined as $H = \lambda_1 f_1 + \lambda_2 f_2 + \lambda_3 f_3 + \lambda_4 f_4$ and the variation principle of optimal control is followed. To achieve a stationary point, the stationary condition must therefore finally be imposed:

$$\frac{\partial H}{\partial u} = p_2 = 0 \tag{7}$$

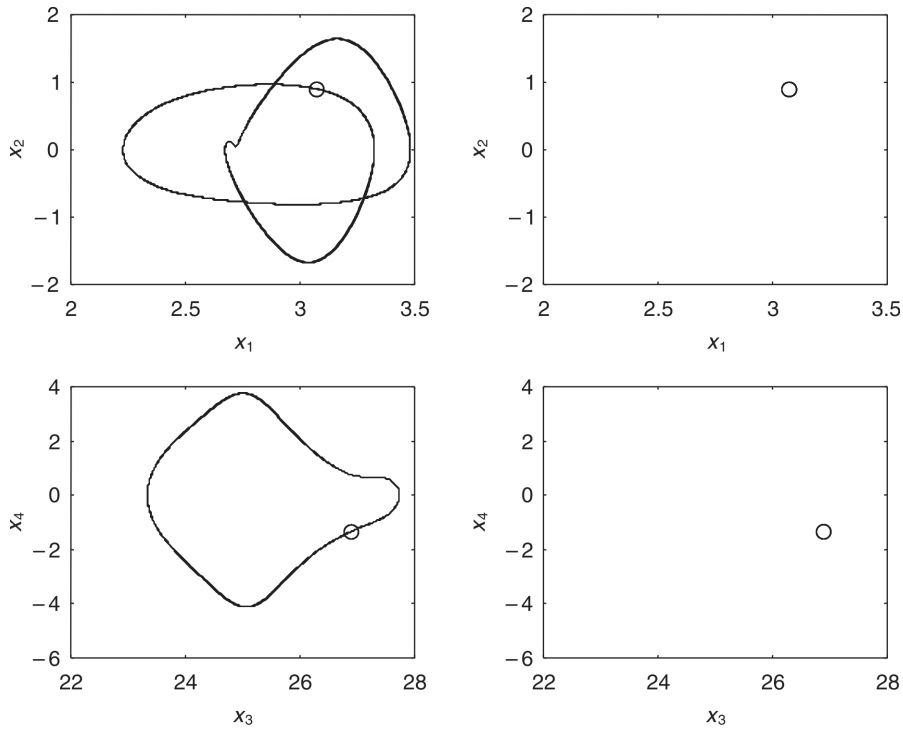

Fig. 16 Phase portraits and the Poincaré map of period 1 for $k_b = 2$

and

$$p_1 x_2 + p_2 f_2 + p_3 x_4 = 0$$
$$-\frac{\partial f_4}{\partial x_4} p_4 = \left[\frac{2\sin x_3' \cos x_3'}{a - \cos^2 x_3'} x_4 + \frac{ak_1}{\Omega m_B \ell^2 (a - \cos^2 x_3')}\right] p_4 = 0 \tag{8}$$

This yields a non-trivial solution for (p_1, p_3, p_4) if and only if

$$\frac{2\sin x_3' \cos x_3'}{a - \cos^2 x_3'} x_4 + \frac{ak_1}{\Omega m_B \ell^2 (a - \cos^2 x_3')} = 0 \tag{9}$$

This gives an optimal surface singularly in the state space. This type of control assumes values on the two allowable boundaries (7) and (8) alternatively, according to a switching surface. Locating system trajectories on the surface, a typical feedback control in the form

$$u = -k_b \operatorname{sgn}\left[\frac{2\sin x_3' \cos x_3'}{a - \cos^2 x_3'} x_4 + \frac{ak_1}{\Omega m_B \ell^2 (a - \cos^2 x_3')}\right]$$

can be used. The sgn function has the following style:

$$\operatorname{sgn}[v] = \begin{cases} +1 & \text{if } v > 0 \\ 0 & \text{if } v = 0 \\ -1 & \text{if } v < 0 \end{cases}$$

For $k_b = 2$, the phase portraits and Poincaré map are shown in Fig. 16 for period 1.

5.6 Control of chaos by the adaptive control algorithm

An adaptive control algorithm utilizes an error signal proportional to the difference between the goal output and the actual output of the system. Generally speaking, an adaptive controller is one that has adjustable parameters and the capability of self-adjusting these parameters in response to changes within the dynamics and environment of the controlled system. The system motion is set back to a desired state x_s by adding dynamics on the control parameter p through the evolution equation

$$\dot{p} = \varepsilon R(x - x_s) \tag{10}$$

where R could be either linear or non-linear and ε indicates the stiffness of the control. In order to convert the dynamics of system (3) from chaotic motion to a desired motion x_s, parameter A is chosen to be perturbed as

$$\dot{A} = \varepsilon[(x_1 - x_{s1})(x_2 - x_{s2})(x_3 - x_{s3})] \tag{11}$$

Then the system can reach the desired periodic trajectory shown as Fig. 17 with $\varepsilon = 0.16$ for period 1.

5.7 Control of chaos by periodic parametric forcing

One of the early studies on parameter-dependent approaches to chaos control focuses on the possible effect of a periodic variation of some system parameter

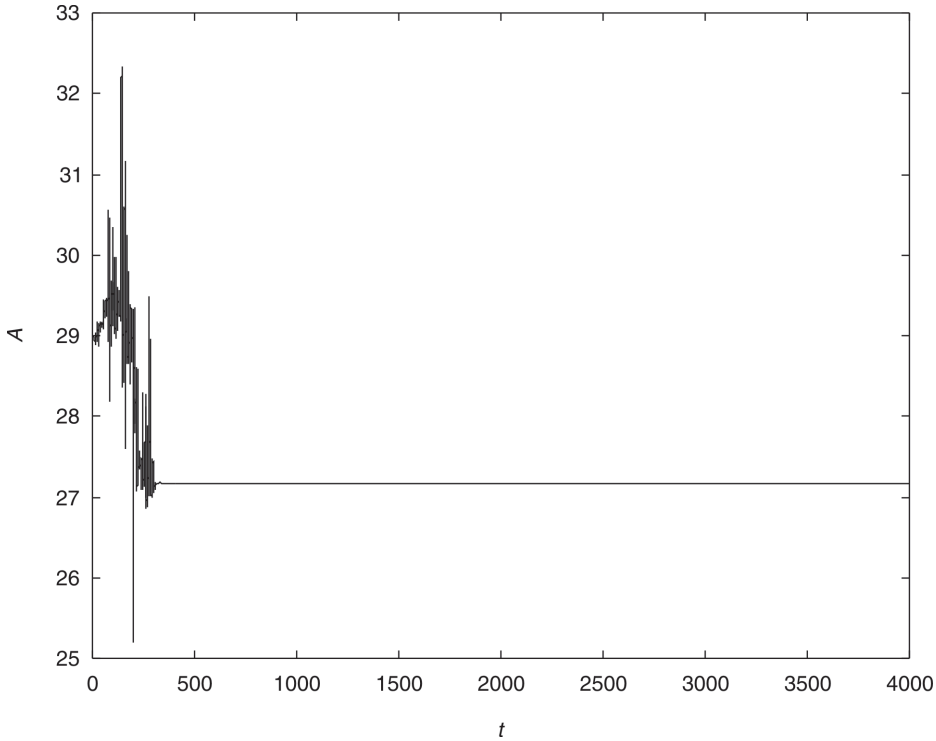

Fig. 17 Time history of adaptive control for A of period 1

in modifying the dynamics of a system with a strange attractor and directly reducing or suppressing chaos. The suggestion of such a possible effect is based on the observation that parametric excitation can stabilize unstable equilibria of linear or linearized systems.

First $k_2 \to k_2[1 + c\sin(\Omega_p \tau)]$ is considered where c is a constant. This type of coupling of weak periodic oscillations to a control parameter can be quite effective when applied to chaotic systems. The interesting consequence of varying the parameter k_2 to $k_2[1 + c\sin(\Omega_p \tau)]$ can be observed from $\Omega_p - \lambda$ (maximum Lyapunov exponent) shown in Fig. 18. The suppression of chaos occurs ($\lambda = 0$) when Ω_p is 5.

6 CHAOS SYNCHRONIZATION

Chaos synchronization has increasing potential for applications. In conventional communication systems, sinusoidal signals are used as carriers, which normally offer excellent bandwidth efficiency. However, their transmitted power is concentrated within a narrow band, resulting in high power spectral density. Then, it may lead to loss of synchronization, high interception possibilities, etc. On the contrary, chaotic signals are usually broadband and noiselike. Hence, synchronized chaotic systems can be used as cipher generators for secure communication [**15**], symmetry and pattern formation and self-organization [**16**–**18**].

There are many effective methods that can be used for chaos synchronization. It is achieved by adding a single coupled term and detected by the Lyapunov exponent. In this paper, synchronization of feedback methods in two identical non-autonomous coupled systems has been studied. Then the phase effect of external excitations of two coupled systems [**19**] has also been researched.

6.1 Feedback synchronization

Synchronization of the two coupled systems can be understood from a feedback control point of view, as follows:

$$\begin{aligned} \dot{x}_1 &= f_1 \\ \dot{x}_2 &= f_2 \\ \dot{x}_3 &= f_3 - \varepsilon(x_3 - x_7) \\ \dot{x}_4 &= f_4 \end{aligned} \tag{12}$$

$$\begin{aligned} \dot{x}_5 &= f_5 \\ \dot{x}_6 &= f_6 \\ \dot{x}_7 &= f_7 + \varepsilon(x_3 - x_7) \\ \dot{x}_8 &= f_8 \end{aligned} \tag{13}$$

where equations (12) and (13) are identical systems but

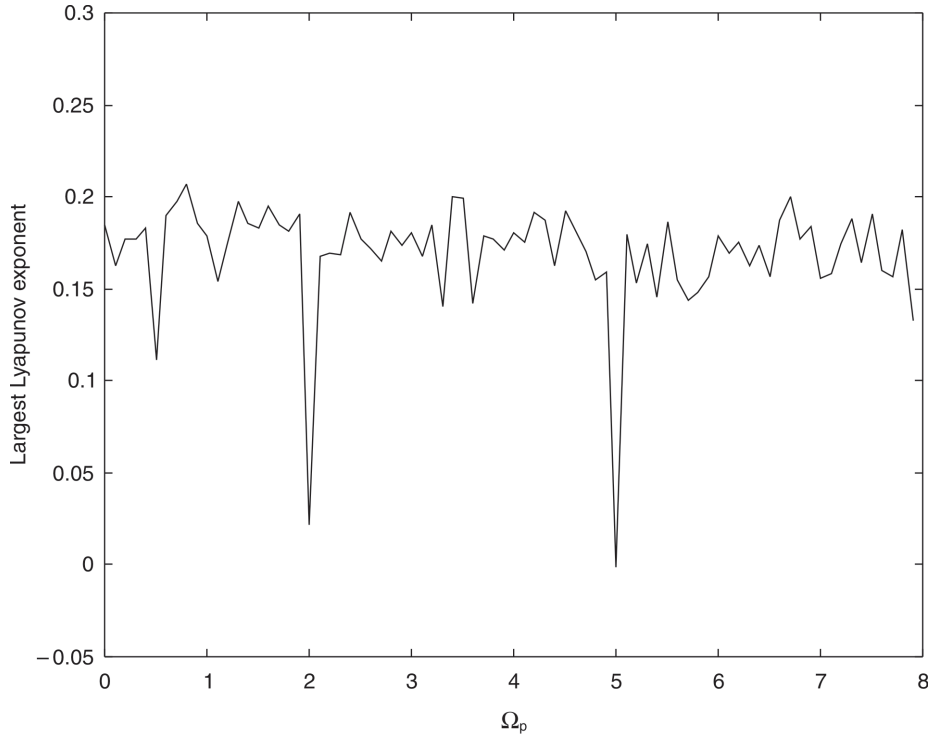

Fig. 18 The largest Lyapunov exponent for Ω_p between 0 and 8

have different initial conditions. From Figs 19 to 21, it can be seen that the two coupled systems are synchronized. Changing $\varepsilon(x_3 - x_7)$ to $\varepsilon \sin(x_3 - x_7)$ and $(e^{\varepsilon(x_3-x_7)} - 1)$, the same results can also be seen in Figs 19 to 21. Then, $\varepsilon(x_3 - x_7)$ is taken as an example. In Fig. 22, it can be seen that if ε exceeds 0.6, synchronization can always be achieved. In Fig. 23, when $\varepsilon = 0.6$ one of the Lyapunov exponents transverses the zero value from positive to negative. This indicates that transversality means synchronization. In Fig. 24, when ε becomes larger, the time to achieve synchronization becomes smaller.

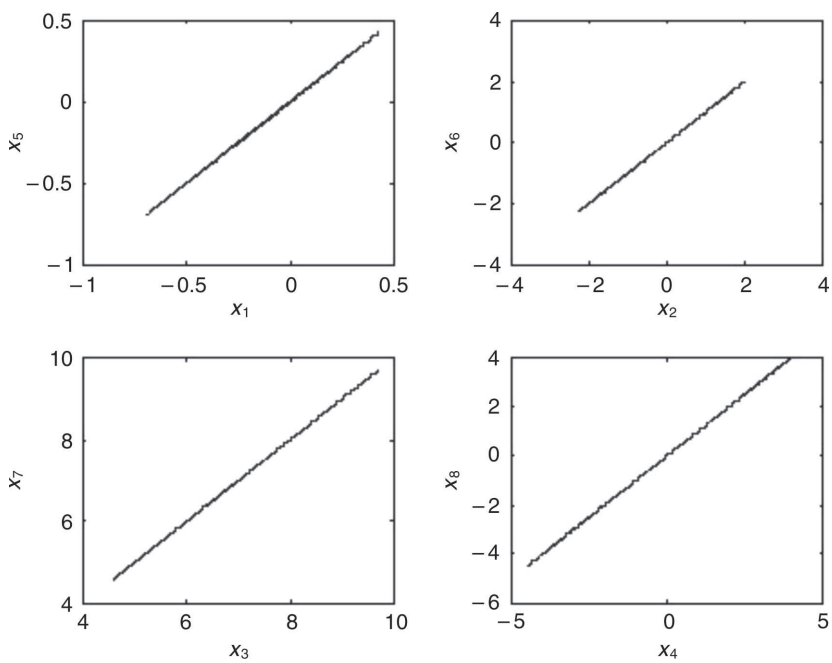

Fig. 19 Synchronized submanifolds of coupled systems with coupling $\varepsilon(x_3 - x_7), \varepsilon = 1$

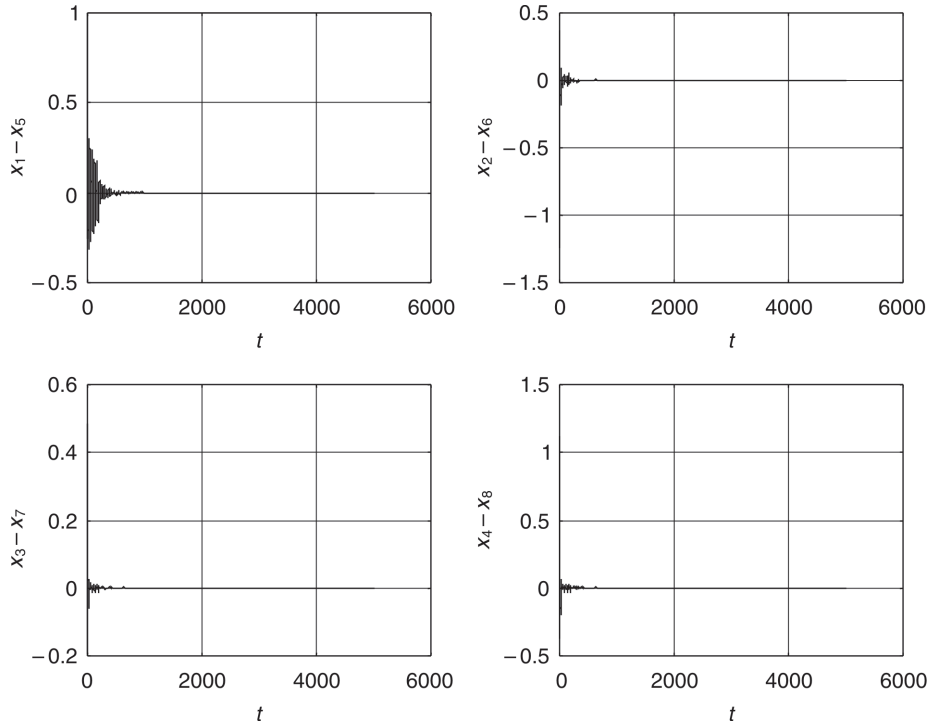

Fig. 20 Errors of two coupled systems with $\varepsilon(x_3 - x_7), \varepsilon = 1$

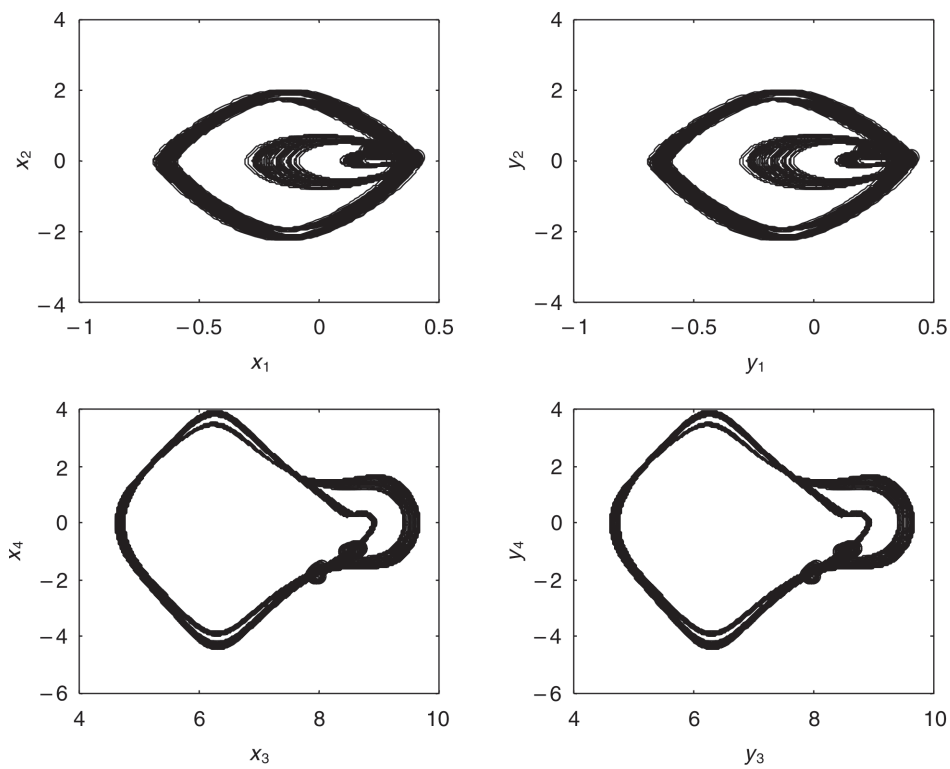

Fig. 21 Phase portraits of two coupled systems with $\varepsilon(x_3 - x_7), \varepsilon = 1$

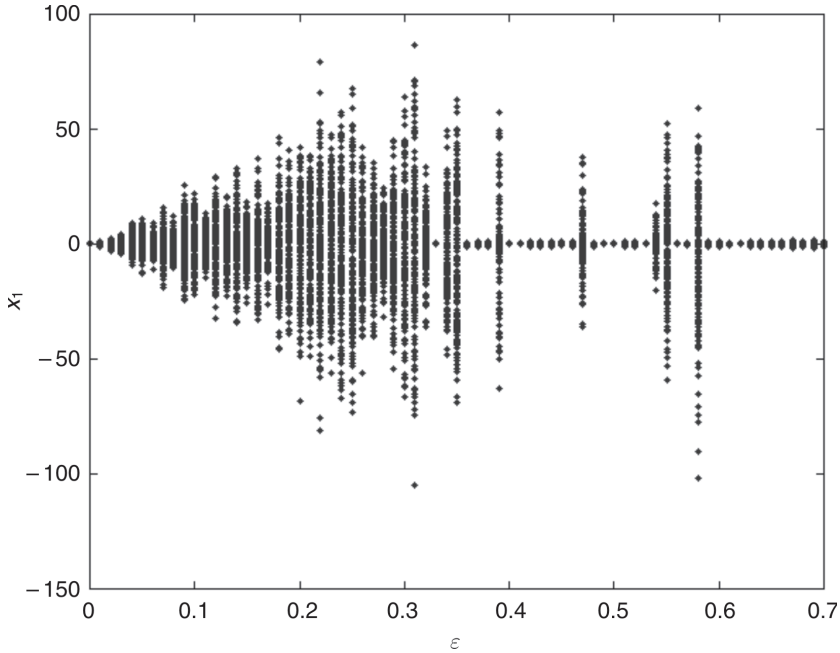

Fig. 22 Bifurcation diagram for ε between 0 and 1 versus x_1

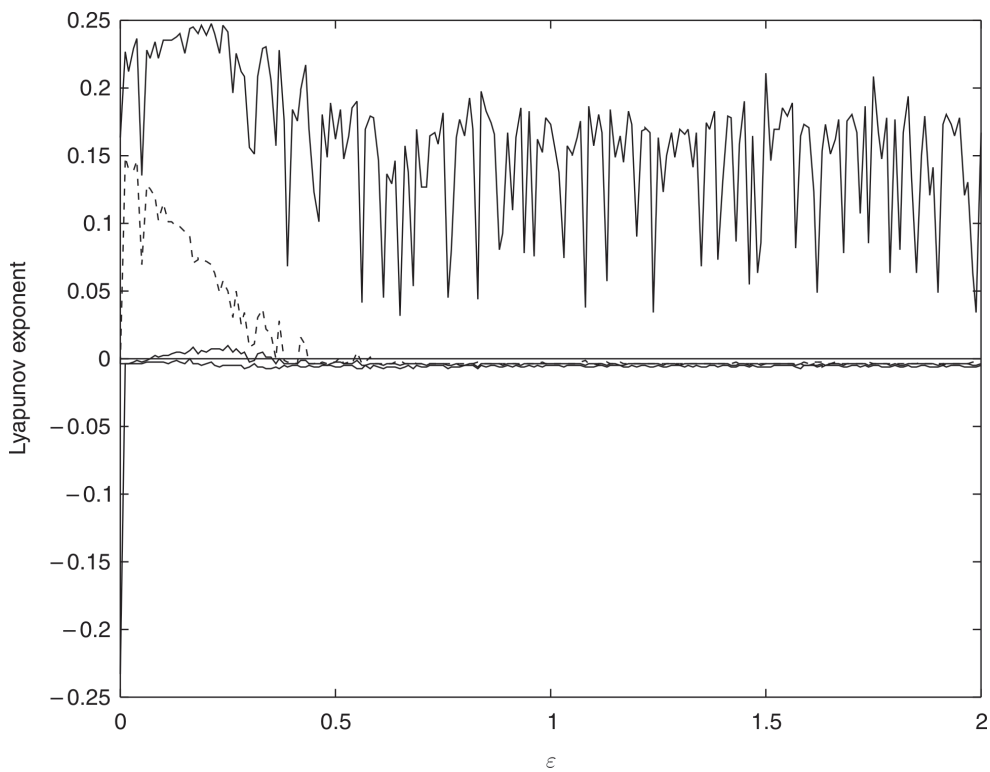

Fig. 23 The Lyapunov exponent for ε between 0 and 1

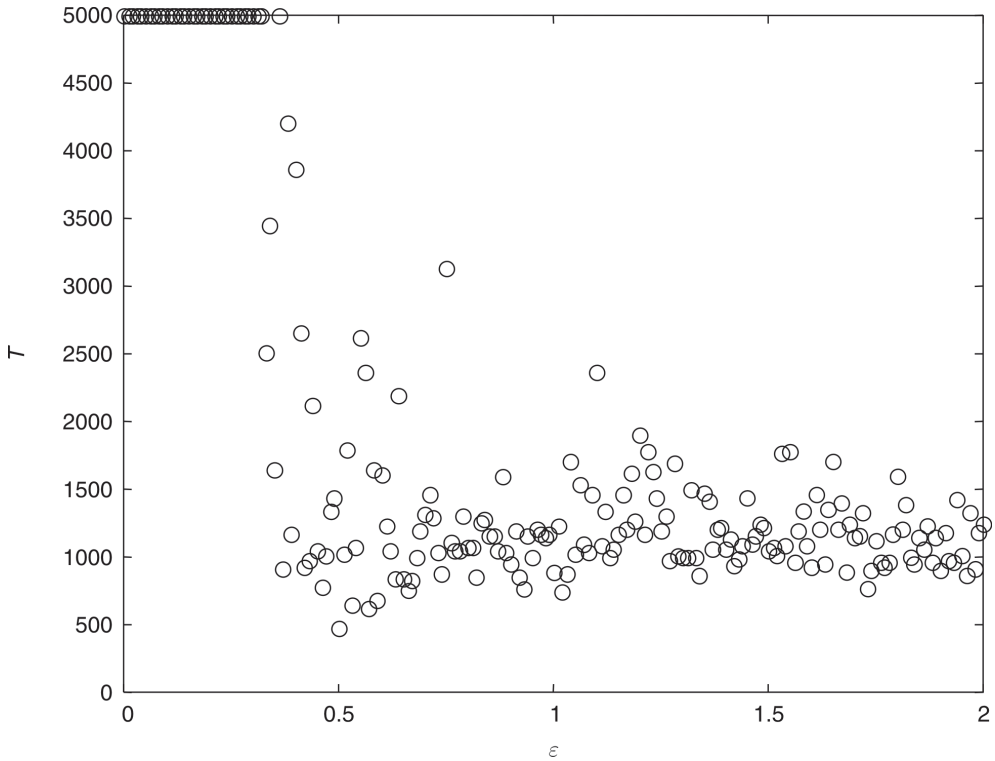

Fig. 24 Synchronization time for different ε

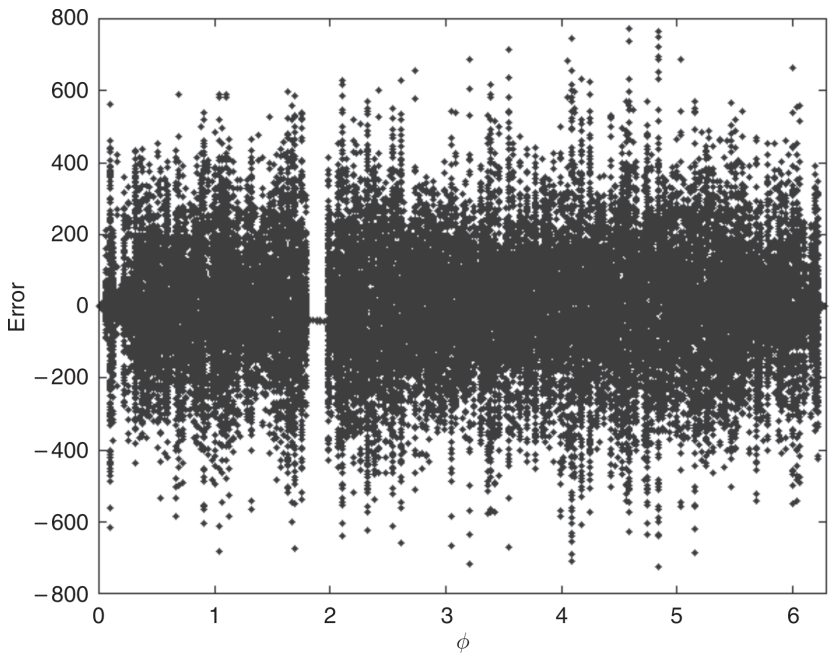

Fig. 25 Diagram for ϕ between 0 and 2π versus error

6.2 Phase effect of two external excitations for two coupled systems

The phase difference between the two external excitations may affect chaos synchronization. Recently, it has been shown that the phase difference between two externally driven forces can play an important role in the driven systems [**20**, **21**]. Now, the systems become

$$\begin{aligned}\dot{x}_1 &= f_1\\ \dot{x}_2 &= f_2(x_1, x_2, x_3, x_4, \sin(\omega\tau))\\ \dot{x}_3 &= f_3 - \varepsilon(x_3 - x_7)\\ \dot{x}_4 &= f_4(x_1, x_2, x_3, x_4, \sin(\omega\tau))\end{aligned} \tag{14}$$

$$\begin{aligned}\dot{x}_5 &= f_5\\ \dot{x}_6 &= f_6(x_5, x_6, x_7, x_8, \sin(\omega\tau + \phi))\\ \dot{x}_7 &= f_7 + \varepsilon(x_3 - x_7)\\ \dot{x}_8 &= f_8(x_5, x_6, x_7, x_8, \sin(\omega\tau + \phi))\end{aligned} \tag{15}$$

where ϕ is the phase difference of external excitation and ω is the external excitation. Then $\omega = 1$ is selected. In Fig. 25, $x_1 - x_5$ versus ϕ is shown with the coupling strength $\varepsilon = 1$. The corresponding Lyapunov exponents of the responses of the non-linear dynamical system are plotted in Fig. 26.

To determine the level of the mismatch of chaos synchronization quantitatively, a similarity function $S(\sigma)$ is used as a time-averaged difference between the variables x_1 and x_5 taken with the time drift σ [**22**], and the similarity function $S(0)$ versus ϕ is plotted in Fig. 27. This shows that at $\phi = 0, S(0)$ is zero. When ϕ becomes large, the mismatch increases at first, then keeps around 2, when $\phi = 2\pi$, and $S(0)$ becomes zero again. Thus

$$S^2(\sigma) = \frac{\langle [x_1(\tau + \sigma) - x_5(\tau)]^2 \rangle}{[\langle x_1^2(\tau)\rangle \langle x_5^2(\tau)\rangle]^{1/2}}$$

In Fig. 28, $S(\sigma)$ versus σ is plotted using different coupling strengths ε. When $\varepsilon > 0.6, S_{\min}$, a minimum of $S(\sigma)$, appears to be zero.

Above all, the phase effect of the two mutually coupled systems have been considered. The phase difference plays an important role. It destroys the complete synchronization of two coupled systems even if it is a small value. Then synchronization is achieved again at $\phi = 2\pi$.

7 CONCLUSIONS

In this paper, the dynamic system of the vibrometer exhibits regular and chaotic behaviour as the parameters are varied. In sections 3 and 4, computational analyses have been studied. Considering the system to be non-autonomous, the periodic and chaotic motions are

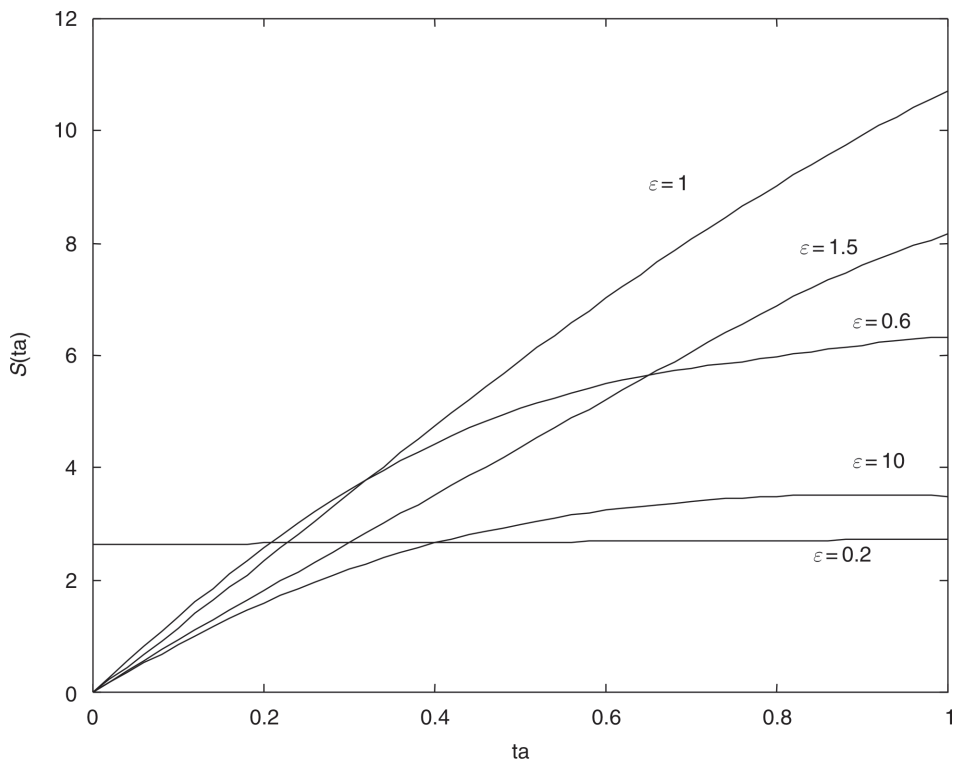

Fig. 26 Similarity function $S(\sigma)$ versus the different strength ε

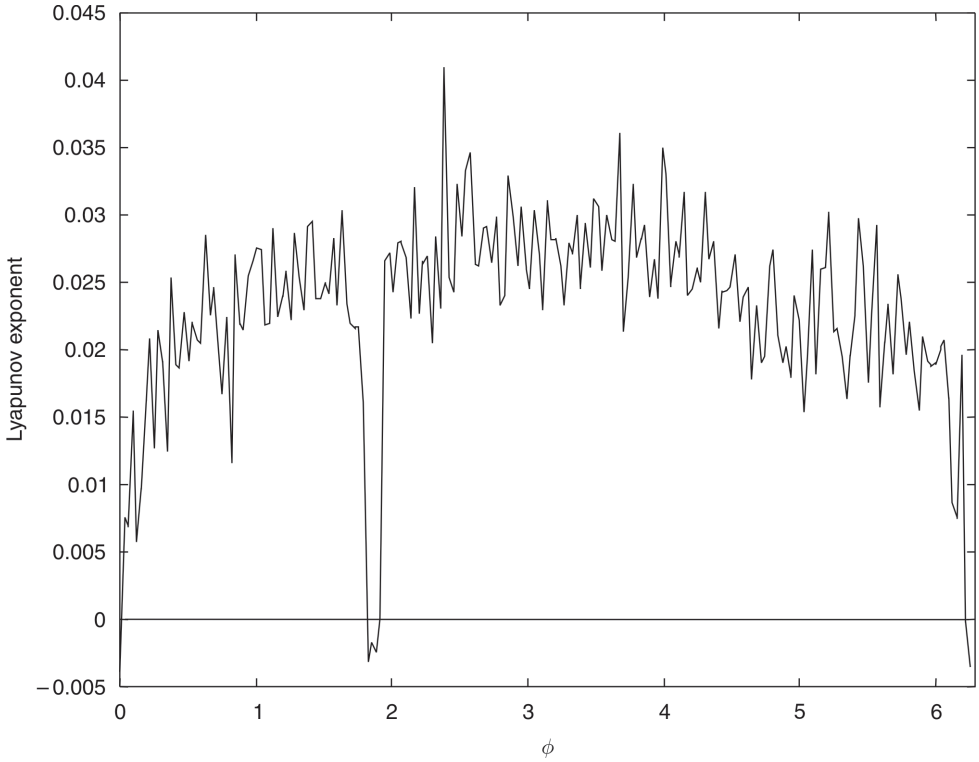

Fig. 27 The Lyapunov exponent for ϕ between 0 and 2π

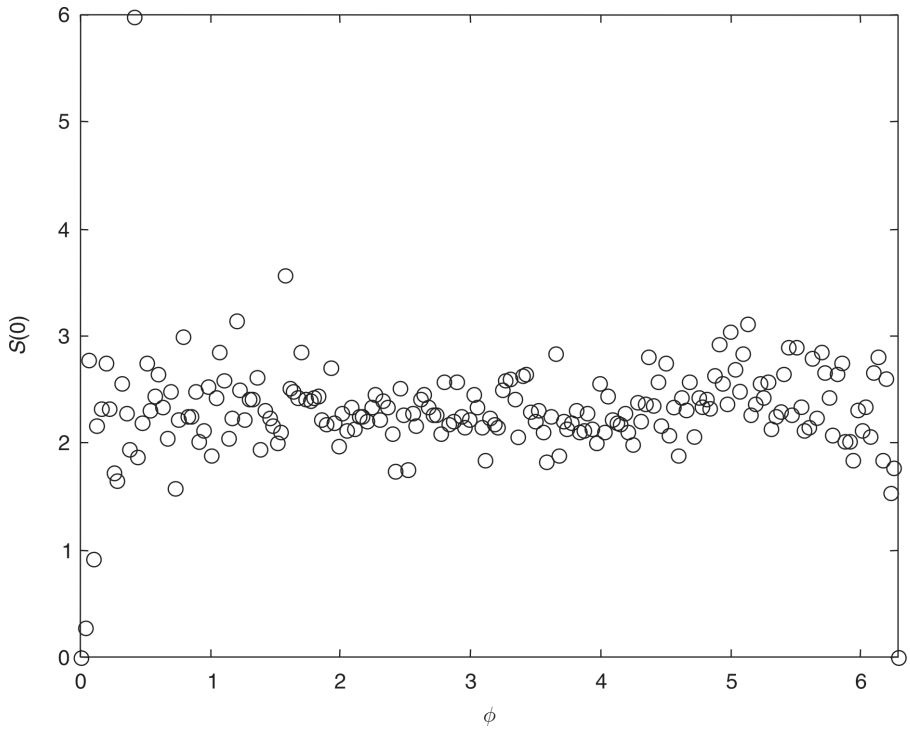

Fig. 28 The similarity function $S(0)$ versus the phase difference ϕ

obtained by numerical methods such as bifurcation, the Poincaré map, Lyapunov exponents and the power spectrum. In addition, a large amount of information of the behaviours of the periodic and chaotic motions can be found in parameter diagrams. The changes of parameter play an important role in the non-linear system. The chaotic motion has been detected using Lyapunov exponents. Though there are some errors

with the results of the computer simulation, the conclusions match the bifurcation diagrams.

Because chaotic motion has a sensitive dependence on the initial condition in deterministic physical systems, a chaotic system must be controlled to yield a periodic motion that is beneficial in working with a particular condition. There are seven control methods that have been studied in section 5. The first three methods of controlling chaos are provided by conventional open-loop control. In the others closed-loop control is used. The delayed feedback control of chaos is a simple way to govern the chaotic system. By setting a delayed signal, the weight of the control signal can easily be adjusted to achieve the stabilization. The optimal control is also useful in suppression of chaos. This method can steer a chaotic trajectory towards a regular trajectory. If the aim is to set the system motion to a desired predetermined regular orbit of the original system, the adaptive control is the sole method among the seven methods given in this paper.

During the past decade, there have been many effective methods that could be used for chaos synchronization. Synchronized chaotic systems can be used as cipher generators for secure communication, symmetry and pattern formation, and self-organization. It is worthy of further research. In section 6, feedback synchronization, one of many effective methods for chaos synchronization, was studied. It can be seen that chaos can be synchronized with some special feedback control and that the phase difference of external excitations affects the synchronization.

ACKNOWLEDGEMENT

This research was supported by the National Science Council, Republic of China, under Grant NSC 92-2212-E-009-027.

REFERENCES

1 **Ge, Z.-M.** *Bifurcation, Chaos and Chaos Control of Mechanical Systems*, 2001 (Gauli Book Company, Taipei, Taiwan).
2 **Ge, Z.-M.** *Bifurcation, Chaos Control for Rigid Body Systems*, 2002 (Gauli Book Company, Taipei, Taiwan).
3 **Thompson, J. M. T.** and **Stewart H. B.** *Nonlinear Dynamics and Chaos*, 2002 (John Wiley, Chichester).
4 **Ott, E.** *Chaos in Dynamical Systems*, 2002 (Cambridge University Press, Cambridge).
5 **Brockett, T. W.** On conditions leading to chaos in feedback system. In Proceedings of the IEEE 21st Conference on *Decision and Control*, 1982, pp. 932–936.
6 **Holmes, P.** Bifurcation and chaos is a simple feedback control system. In Proceedings of the IEEE 22nd Conference on *Decision and Control*, 1983, pp. 365–370.
7 **Chen, G.** and **Yu, X.** (Eds) *Chaos Control, Theory and Application*, 2003 (Springer, New York).
8 **Pyragas, K.** Continuous control of chaos by self-controlling feedback. *Phys. Lett. A*, 1992, **170**, 421–428.
9 **Chen, G.** and **Dong, X.** *From Chaos to Order: Methodologies, Perspectives and Applications*, 1998 (World Scientific, New Jersey).
10 **Sinha, S., Ramaswamy, R.** and **Rao, J. S.** Adaptive control in nonlinear dynamics. *Physica D*, 1991, **43**, 118–128.
11 **Bunner, M. J.** and **Just, W.** Synchronization of time-delay systems. *Phys. Rev. E*, 1998, **58**(4).
12 **Pikovsky, A. S., Rosenblum, M. G., Osipov, G. V.** and **Kurths, J.** Phase synchronization of chaotic oscillators by external driving. *Physica D*, 1997, **104**, 219–238.
13 **Raj, S. P., Rajasekar, S.** and **Murali, K.** Coexisting chaotic attractors, their basin of attractions and synchronization of chaos in two coupled duffing oscillators. *Physics Lett. A*, 1999, **264**, 283–288.
14 **Ianstiti, M., Hu Q., Westervelt, R. M.** and **Tinkham M.** Noise and chaos in a fractal basin boundary regime in a Josephson junction. *Phys. Rev. Lett.*, 1985, **55**, 746–749.
15 **Kocarev, L.** General approach for chaotic synchronization with applications to communication. *Phys. Rev. Lett.*, **74**(25).
16 **Lakshmanan, M.** and **Murali, K.** *Chaos in Nonlinear Oscillators: Controlling and Synchronization*, 1966 (World Scientific, Singapore).
17 **Pikovsky, A. S., Rosenblum, M. G.** and **Kurths, J.** *Synchronization, A Universal Concept in Nonlinear Sciences*, 2003 (Cambridge University Press, Cambridge).
18 **Awrejcewicz, J.** *Bifurcation and Chaos in Coupled Oscillators*, 1991 (World Scientific, Singapore).
19 **Yin, H.-W.** and **Dai, J.-H.** Phase effect of two coupled periodically driven duffing oscillators. *Phys. Rev. E*, 1998, **58**(5).
20 **Chacón, R.** Geometrical resonance as a chaos eliminating mechanism. *Phys. Rev. Lett.*, 1996, **77**(3).
21 **Qu, Z., Hu, G., Yang, G.** and **Qin, G.** Phase effect in taming nonautonomous chaos by weak harmonic perturbations. *Phys. Rev. Lett.*, 1995, **74**.
22 **Rosenblum, M. G., Pikovsky, A. S.** and **Kurths, J.** From phase to lag synchronization in coupled chaotic oscillators. *Phys. Rev. Lett.*, 1997, **78**.